

Ground-state properties via machine learning quantum constraints

Pei-Lin Zheng[#], Si-Jing Du[#], and Yi Zhang^{*}

*International Center for Quantum Materials, Peking University, Beijing, 100871, China and
School of Physics, Peking University, Beijing, 100871, China*

Ground-state properties are central to our understanding of quantum many-body systems. At first glance, it seems natural and essential to obtain the ground state before analyzing its properties; however, its exponentially large Hilbert space has made such studies costly, if not prohibitive, on sufficiently large system sizes. Here, we propose an alternative strategy based upon the expectation values of an ensemble of selected operators and the elusive yet vital quantum constraints between them, where the search for ground-state properties simply equates to classical constrained minimization. These quantum constraints are generally obtainable via sampling then machine learning on a large number of systematically consistent quantum many-body states. We showcase our perspective on 1D fermion chains and spin chains for applicability, effectiveness, and several unique advantages, especially for strongly correlated systems, thermodynamic-limit systems, property designs, etc.

Introduction—The collective behaviors of quantum many-body systems are central to various cutting-edge fields in condensed matter physics and beyond. Despite the nominal simplicity of certain quantum Hamiltonians, e.g., the Hubbard model [1–3], the non-commuting quantum operators squander any advantageous basis, and the exponentially-large Hilbert space renders the solutions and characterizations of ground states costly, limiting the system size and geometry in numerical techniques, e.g., exact diagonalization and density matrix renormalization group (DMRG) [4, 5]. While quantum Monte Carlo methods introduce efficient samplings, they are limited to sign-problem-free cases [6–8]. Also, the ground state solution usually starts from scratch upon slight model modifications, making the systematic study of a complex phase diagram, not uncommon in condensed matter physics [9], even more expensive.

Rather than the abstract quantum many-body ground state, we are usually interested in its properties such as ground-state energy and spontaneous-symmetry-breaking order parameters - (linear combinations of) expectation values of target observables. Considering that the minimum energy criteria also concerns expectation values, one would be prompt to establish a study based solely upon the expectation values and cut out the ground state. However, the quantum operators follow nontrivial commutation relations, and as a result, enforce nontrivial quantum constraints upon their expectation values - a role played by the ground state as the mediator. Expectation values violating these quantum constraints do not have an underlying quantum state and may not reflect the true nature of the quantum many-body system. Therefore, these convoluted quantum constraints are essential for expectation-value-based considerations.

On the other hand, recent developments in machine learning [10, 11] have revolutionized data analysis such as image recognition, spam and fraud detection, and autonomous driving [12]. Artificial neural networks (ANNs) can grasp the key yet complex and hidden rules in big datasets and decide accurately for future scenarios [10–

12]. Recently, machine learning has witnessed many explorations at the quantum many-body physics frontier, including quantum state tomography [13, 14], quantum phase recognition [15–22], neural-network states [23, 24], experiment interpretations [25–27], etc.

In this letter, we propose to study the ground-state properties of quantum many-body systems within a classical expectation-value framework with quantum constraints over an ensemble of relatively important operators. With these quantum constraints, the ground state properties amount to constrained minimization. In general, we can express such quantum constraints in terms of ANNs and extract them from quantum state examples via supervised machine learning. Without loss of generality, we consider 1D fermion models and spin-1/2 models to showcase our strategy, which has unique advantages: (1) Compared with the expensive procedure of solving quantum many-body states, evaluations of expectation values are efficient and easily parallelizable for multiple operators and states. (2) Our main bottleneck is the extraction and application of the quantum constraints through a large, classical dataset of expectation values, which modern machine learning techniques excel compatibly and proficiently. (3) The obtained quantum constraints work for all Hamiltonians in a phase diagram and beyond, where one iterates the constrained minimization with respect to the expectation values. (4) We embed systematic properties such as system size, geometry, and dimensions into the sample quantum many-body states and are rarely limited by them. For instance, we can target ground-state properties in the thermodynamic limit directly without the need for finite-size extrapolations. (5) The quantum constraints also exhibit the competition and symbiosis between the observables explicitly, offering recipes for engineering Hamiltonians for desired ground-state properties and emergent phases.

Algorithm—Our approach consists of steps as follows:

- Start with a large and representative ensemble of quantum many-body states $\{|\Phi\rangle_\alpha\}$ with systemat-

ically consistent with the potential ground state.

- For each $|\Phi\rangle_\alpha$, evaluate the expectation values of a set of selected operators $\{\hat{O}_j\}$ and contribute a sample point $\langle\hat{\mathbf{O}}\rangle_\alpha = (\langle\hat{O}_1\rangle_\alpha, \langle\hat{O}_2\rangle_\alpha, \dots)$ in the $\langle\hat{\mathbf{O}}\rangle$ space. Operators with lower orders and spatial extents get higher priority due to their larger relevance and expectation values.
- Via supervised machine learning on the training set $\{\langle\hat{\mathbf{O}}\rangle_\alpha\}$, train ANNs $f(\langle\hat{\mathbf{O}}\rangle)$ to distinguish physical (unphysical) values of $\langle\hat{\mathbf{O}}\rangle$ that is allowed (disallowed) by the quantum constraints.
- For the Hamiltonian $H = \sum_j a_j \hat{O}_j$, search the constrained minimum of the energy $E = \sum_j a_j \langle\hat{O}_j\rangle$ with the quantum constraints $f(\langle\hat{\mathbf{O}}\rangle)$. The coordinates $\langle\hat{\mathbf{O}}\rangle_0$ of the resulting minimum offer the expectation values that characterize the ground state.

Further, the adiabatic theorem ensures that the quantum many-body ground states and the corresponding $\langle\hat{\mathbf{O}}\rangle_0$ evolves continuously with the Hamiltonian in the absence of first-order phase transitions. We can start with models with exact solutions or controlled approximations and progressively tune the Hamiltonians into other parts of the phase diagram with $\langle\hat{\mathbf{O}}\rangle_0$ tracked down successively during the constrained minimization processes [28].

A heuristic example—First, let's consider a 1D Fermi sea, where we have a simple expression for the quantum constraints. For quantum many-body states with a single Fermi sea between $k_L = k_0 - k_F$ and $k_R = k_0 + k_F$ [28], the expectation values of two-point correlators are:

$$\begin{aligned} C_0 &= \langle c_x^\dagger c_x \rangle = k_F / \pi \\ C_r &= \langle c_{x+r}^\dagger c_x \rangle = \sin(k_F r) e^{ik_0 r} / \pi r, r \neq 0, \end{aligned} \quad (1)$$

irrespective of x due to the translation symmetry. Expectation values of higher-order operators depend fully on C_r 's through Wick's theorem. In particular, the following quantum constraint holds between the most dominant real-valued C_0 and complex-valued C_1 :

$$\pm \pi |C_1| = \sin(\pi C_0), \quad (2)$$

as illustrated in Fig. 1. As long as there is one Fermi sea and no spontaneous translation symmetry breaking, the quantum constraint holds irrespective of Hamiltonian.

Now, let's consider a tight-binding Hamiltonian with nearest-neighbor hopping $t \in \mathbb{R}$ [29] and Fermi energy μ :

$$\begin{aligned} H &= \sum_x -t(c_{x+1}^\dagger c_x + c_x^\dagger c_{x+1}) + \mu c_x^\dagger c_x \\ E &= (-2t \text{Re}(C_1) + \mu C_0) \times N, \end{aligned} \quad (3)$$

where N is the system size, and we set $t = 1$ as our unit of energy hereinafter. As the constraint in Eq. 2 only concerns $|C_1|$, we need to set $\text{Im}(C_1) = 0$ to minimize E .

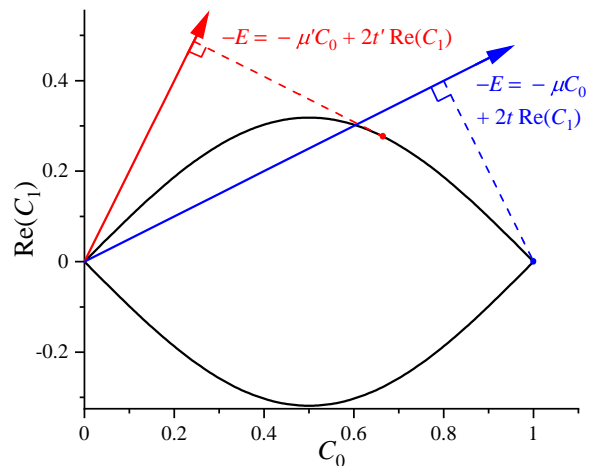


FIG. 1. The black contour shows the values of $(\text{Re}(C_1), C_0)$ consistent with the quantum constraint in Eq. 2 for $\text{Im}(C_1) = 0$. Those expectation values not on the contour are unphysical, i.e., there is no quantum many-body state to realize them. The coordinates of the point on the contour with the lowest energy expectation value, projected along different directions for different Hamiltonians, e.g., $t = 1, \mu = -4$ (blue) and $t' = 1, \mu' = -1$ (red), characterize the ground-state properties.

A schematic plot for the optimal values of $(\text{Re}(C_1), C_0)$ is in Fig. 1. More rigorously, we define $\pi C_0 = y \in (0, \pi)$, and $\text{Re}(C_1)/C_0 = f(y) = \sin(y)/y \in (0, 1)$ is a single-valued function following the quantum constraint. To minimize $E \propto [\mu - 2tf(y)] \times y$, the subsequent solutions:

$$\begin{aligned} 2tf(y) - \mu + 2tf'(y)y &= 0 \Rightarrow 2t \cos(y) = \mu \\ C_0 &= y/\pi = \arccos(\mu/2t)/\pi \\ \text{Re}(C_1) &= yf(y)/\pi = \sin(y)/\pi = \text{sgn}(t) \sqrt{1 - \mu^2/4t^2}/\pi \end{aligned} \quad (4)$$

are consistent with the exact results obtained in the momentum space $H = \sum_k [-2t \cos(k) + \mu] c_k^\dagger c_k$ for generic values of t and μ .

For ground-state properties of Hamiltonians with upto n^{th} -nearest-neighbor hopping, we need to employ quantum constraint $C_0 = f(C_1/C_0, C_2/C_0, \dots)$ on the expectation values $C_i, i = 0, 1, 2, \dots, n_{fs}$, which can be represented by ANNs and trained via supervised machine learning on quantum states with multiple Fermi seas [28]. For general quantum many-body systems, we may not formulate the quantum constraints as a function between the expectation values. It will be more convenient to establish a 'penalty' function $f(\langle\hat{\mathbf{O}}\rangle)$ that measures the extent of violations of $\langle\hat{\mathbf{O}}\rangle$ to the quantum constraints, which we examine the next.

Benchmark examples—We consider 1D fermion insulators with a bipartite unit cell, whose Bloch states have a general form $u(k) = (\cos(\theta_k/2), \sin(\theta_k/2) \exp(i\varphi_k))^T$, where the first (second) component denotes the A (B) sublattice. The expectation values of two-point correla-

tors are:

$$\begin{aligned} C_0^{AA(BB)} &= 0.5 \pm g_0/2, \\ C_r^{AA(BB)} &= \pm g_r/2, r \in \mathbb{Z}^+, \\ C_{r'}^{AB} &= \tilde{g}_{r'}/2, r' \in \mathbb{Z} + 1/2, \end{aligned} \quad (5)$$

and the rest can be obtained via complex conjugation. The following quantum constraints are present over $g_r = \int_0^{2\pi} \frac{dk}{2\pi} e^{ikr} \cos(\theta_k)$ and $\tilde{g}_{r'} = \int_0^{2\pi} \frac{dk}{2\pi} e^{i(kr'+\varphi_k)} \sin(\theta_k)$:

$$\sum_r g_r \cdot g_{r+s}^* + \sum_{r'} \tilde{g}_{r'} \cdot \tilde{g}_{r'+s}^* = \delta_s. \quad (6)$$

g_r and $\tilde{g}_{r'}$, related to correlations in insulators, are fast decaying functions of r and r' , which allows us to truncate at a finite distance $\Lambda = 10$ unless noted otherwise. We define a positive-definite penalty function:

$$f(g_r, \tilde{g}_{r'}) = \sum_{s=0}^{\Lambda/2} \left[\sum_r g_r \cdot g_{r+s}^* + \sum_{r'} \tilde{g}_{r'} \cdot \tilde{g}_{r'+s}^* - \delta_s \right]^2 \quad (7)$$

which yields ~ 0 if and only if $\{g_r, \tilde{g}_{r'}\}$ are consistent with the quantum constraints. We note that the derivation of an expression as Eq. 7 is unavailable in generic quantum scenarios. Here for non-interacting fermions, it offers benchmarks to our strategy via machine learning quantum constraints in the following paragraphs.

Starting from random $u(k)$, we obtain 6.4×10^5 samples of $\{g_r, \tilde{g}_{r'}\}$ consistent with the quantum constraints and no penalty. We also include 2.56×10^6 contrasting samples with small, random deviations added to $\{g_r, \tilde{g}_{r'}\}$ and penalty proportional to the square of the weighted average deviations in the dataset [28]. Besides, we utilize the gauge equivalence to reduce the degrees of freedom [28]. Then, we apply supervised machine learning [10, 11] to train ANNs on the quantum constraints of $\{g_r, \tilde{g}_{r'}\}$ in the neighborhood of small or no violations [28]. In practice, we use the average output of multiple independent ANNs $f^*(g_r, \tilde{g}_{r'})$ as the approximate penalty, and their max output as an acceptance threshold to avoid unphysical regions.

To test out these quantum constraints, we study the mean-field solutions of a 1D interacting fermion Hamiltonian at half-filling:

$$H = \sum_x -t(c_{x+1}^\dagger c_x + c_x^\dagger c_{x+1}) + V c_{x+1}^\dagger c_{x+1} c_x^\dagger c_x. \quad (8)$$

The underlying assumptions of $f(g_r, \tilde{g}_{r'})$ and $f^*(g_r, \tilde{g}_{r'})$ are that the ground state takes a non-interacting fermion framework hence the Hartree-Fock approximation, and an emergent bipartite order parameter may or may not spontaneously break the translation symmetry. Under these circumstances, the energy expectation value is:

$$\begin{aligned} E = \langle H \rangle &= [-t (\text{Re}(\tilde{g}_{1/2}) + \text{Re}(\tilde{g}_{-1/2})) \\ &+ 0.25V (2 - 2g_0^2 - |g_1|^2 - |g_{-1}|^2)] \times N/2. \end{aligned} \quad (9)$$

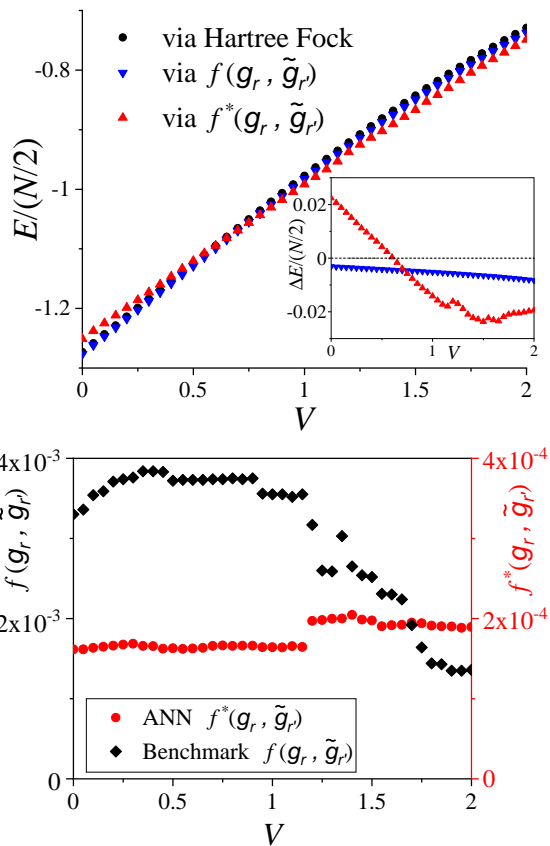


FIG. 2. Top: The ground-state energies and (inset) their relative difference of the quantum many-body system in Eq. 8 from the Hartree Fock approximation as well as the constrained minimization of $L = \bar{E} + \eta f$ and $L = \bar{E} + \eta f^*$, respectively. $\eta = 100$. Note that the energies obtained with our strategy are slightly below the theoretical values since we have slacked the quantum constraints for improved efficiency, except for small V where the mean-field gap diminishes. Bottom: The ANN outputs $f^*(g_r, \tilde{g}_{r'})$ for the constrained minimum as well as the benchmark $f(g_r, \tilde{g}_{r'})$ for the same $\{g_r, \tilde{g}_{r'}\}$ show consistency with the quantum constraints throughout the V range as we gradually lower from $V = 2$.

We look for the constrained minimum $\{g_r, \tilde{g}_{r'}\}$ by minimizing either $L = \bar{E} + \eta f$ or $L = \bar{E} + \eta f^*$, where $\bar{E} = E/(N/2)$, and η controls the weight of the quantum constraints and should balance between values too large to allow an efficient search acceptance rate, and values too small to prevent $\{g_r, \tilde{g}_{r'}\}$ from leaving regions represented by the dataset samples. Also, given the adiabatic theorem and absence of phase transition, we use the expectation values at V as initial points of the search for those at $V + \delta V$, and so on so forth. In practice, we start from $V = 2$ with an interval of $\delta V = -0.05$ [30]. The benchmark results are summarized in Fig. 2 and Ref. [28], and their consistency indicates that machine learning can offer a general and trustworthy path toward quantum constraints.

The quantum-constraint perspective also allows us to

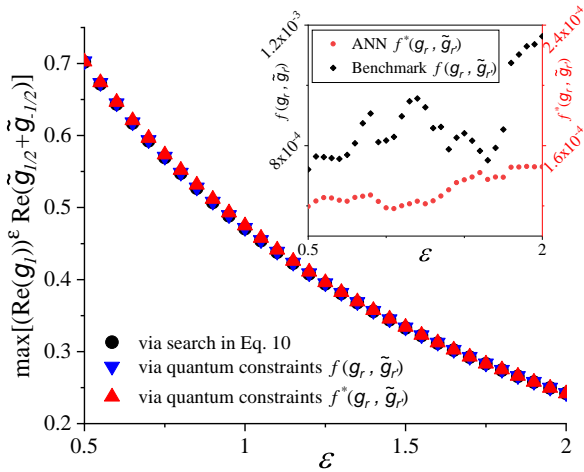


FIG. 3. The maximum of $(\text{Re}(g_1))^\epsilon \text{Re}(\tilde{g}_{1/2} + \tilde{g}_{-1/2})$ for 1D fermion insulators on bipartite lattices shows good consistency between constrained optimization via the quantum constraints and searches among the variational Hamiltonian H_{var} in Eq. 10. Individual expectation values for realizing the maximum, e.g., g_1 and $\tilde{g}_{1/2}$, also check out for each ϵ . For the quantum-constraints approaches, we gradually increase ϵ from $\epsilon = 0.5$ while keeping track of $\{g_r, \tilde{g}_{r'}\}$. Inset: the ANN $f^*(g_r, \tilde{g}_{r'})$ and the benchmark $f(g_r, \tilde{g}_{r'})$ suggest the obtained $\{g_r, \tilde{g}_{r'}\}$ indeed obey the quantum constraints. $\eta = 100$.

design quantum many-body systems like never before. Say we wish to apply certain criteria to expectation values, and sometimes it is as simple as including the corresponding operators into the Hamiltonian, yet sometimes we wish to exclude such operators for nontrivial alternatives, e.g., through spontaneous symmetry breaking, or the criteria simply do not interpret into any operators. For instance, to maximize $(\text{Re}(g_1))^\epsilon \text{Re}(\tilde{g}_{1/2} + \tilde{g}_{-1/2})$, $\epsilon \in [0.5, 2]$ for 1D fermion insulators on bipartite lattices, we simply solve the constrained maximization with the quantum constraints. Conventionally, we need to study a variational Hamiltonian instead, such as:

$$H_{var} = \sum_x -t(c_{x+1}^\dagger c_x + \text{h.c.}) + (-1)^x \Delta (c_{x+2}^\dagger c_x + \text{h.c.}), \quad (10)$$

where Δ is a variational parameter to explore. We compare our results in Fig. 3. While H_{var} balances operators favoring $\text{Re}(\tilde{g}_{1/2} + \tilde{g}_{-1/2})$ and $\text{Re}(g_1)$ for simplicity, larger variational spaces with additional operators are required for thoroughness in general. The solutions of ground states may also cause complications. Our strategy circumvents such difficulties.

Strongly correlated scenarios—Generality is another important merit of our strategy, which applies straightforwardly to strongly correlated systems and outshines the conventional methods hanging on the mind-boggling quantum many-body ground states themselves. Since the ground states of local Hamiltonians obey the Area Law, tensor network states [4, 5, 31, 32] offer an effective and

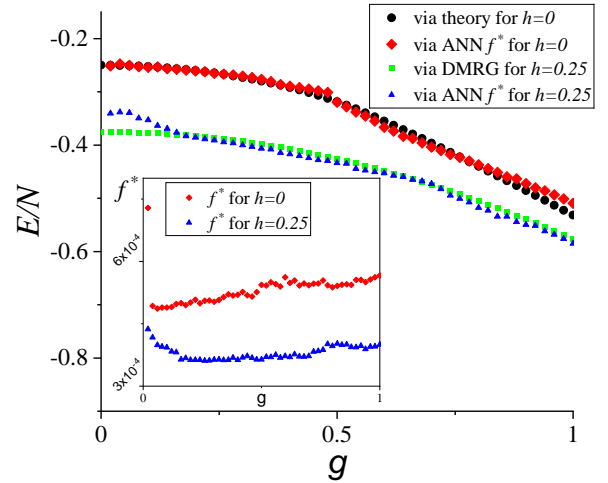


FIG. 4. The ground-state energy of the transverse field Ising model ($h = 0$) and longitudinal-transverse field Ising model ($h = 0.25$) in Eq.11 obtained by theory solutions [33], DMRG, and the constrained minimization using ANN quantum constraints exhibit satisfactory consistency. For the latter, we start from $g = 0$ and gradually increase g . $\eta = 1000/3$ for $h = 0$ and $\eta = 400$ for $h = 2.5$, respectively. Inset: ANN $f^*(\langle \hat{\mathbf{O}} \rangle)$ suggests that the results obey the quantum constraints.

general representation to sample quantum many-body states for machine learning quantum constraints.

Here, we illustrate the quantum constraints of 1D interacting spin-1/2 chains in the thermodynamic limit, represented by infinite matrix product states. First, we sample quantum many-body states with random, translation symmetric matrices of dimension $\chi = 8$. Next, we evaluate the expectation values $\langle \hat{\mathbf{O}} \rangle$ of a series of low-order spin operators S_r^λ and $S_r^\lambda S_{r+l}^{\lambda'}$, $\lambda, \lambda' = x, y, z$ upon a section of length $l_{max} = 6$. Other than 6.75×10^4 of these quantum-constraints-abiding samples, we also include 2.025×10^5 contrasting samples with small deviations and corresponding penalties. Then, we perform supervised machine learning on the dataset and train ANNs $f^*(\langle \hat{\mathbf{O}} \rangle)$ to recognize how well a target $\langle \hat{\mathbf{O}} \rangle$ aligns with the quantum constraints. We note that the trained ANNs, as well as the previous ANNs $f^*(g_r, \tilde{g}_{r'})$ and benchmark $f(g_r, \tilde{g}_{r'})$ for 1D fermion insulators, penalize expectation values' departure from and thereby enforcing the quantum constraints as intended, see Ref. [28].

Subsequently, we use the quantum constraints for ground-state properties of quantum spin Hamiltonians. For instance, we apply our strategy with $f^*(\langle \hat{\mathbf{O}} \rangle)$ to the 1D transverse field Ising model ($h = 0$) as well as the non-integrable longitudinal-transverse field Ising model ($h \neq 0$):

$$H = \sum_j -JS_j^z S_{j+1}^z - gS_j^x - hS_j^z, \quad (11)$$

where we set $J = 1$ as the unit of energy. The results on

the energy expectation value per site $E/N = \langle H \rangle / N = -J \langle S_0^z S_1^z \rangle - g \langle S_0^x \rangle - h \langle S_0^z \rangle$ and beyond in the $N \rightarrow \infty$ thermodynamic limit are summarized in Fig. 4 and the Supplemental Materials [28].

Discussions—We propose to analyze ground-state properties via machine learning quantum constraints on expectation values and complement conventional ground-state-based approaches. Other than the aforementioned advantages, we observe that we have yet established unbiased uncertainties for controlled quantitative analysis, especially for relatively soft degrees of freedom, e.g., the order parameter of a spontaneous symmetry breaking phase [28]. Qualitative tendencies are observable, and an extrapolation of η , the weight of quantum constraints, offers a partial solution [28]. Also, the evaluations of expectation values for tensor network states may become costly in 2D and beyond, thus we also need to consider other quantum-state ansatz. Finally, while the selection of low-order, small-scale operators, the tensor network state representation for quantum-state samples, and the systematic presumptions help narrow down the questions and facilitate the calculations, such physics intuitions and insights should sometimes be taken with a grain of salt.

Acknowledgement: We thank Junren Shi, Xiao Yuan, and Peng-Cheng Xie for insightful discussions. Y.Z. is supported by start-up grant at Peking University. The computation was supported by High-performance Computing Platform of Peking University. The source code and the trained ANNs will be released after publication.

* frankzhangyi@gmail.com; # P.-L. Zheng and S.-J. Du are responsible respectively for 1D fermion chains and spin chains and contributed equally.

- [1] R. T. Scalettar, E. Y. Loh, J. E. Gubernatis, A. Moreo, S. R. White, D. J. Scalapino, R. L. Sugar, and E. Dagotto, *Phys. Rev. Lett.* **62**, 1407 (1989).
- [2] A. Moreo and D. J. Scalapino, *Phys. Rev. Lett.* **66**, 946 (1991).
- [3] J. P. F. LeBlanc, A. E. Antipov, F. Becca, I. W. Bulik, G. K.-L. Chan, C.-M. Chung, Y. Deng, M. Ferrero, T. M. Henderson, C. A. Jiménez-Hoyos, E. Kozik, X.-W. Liu, A. J. Millis, N. V. Prokof'ev, M. Qin, G. E. Scuseria, H. Shi, B. V. Svistunov, L. F. Tocchio, I. S. Tupitsyn, S. R. White, S. Zhang, B.-X. Zheng, Z. Zhu, and E. Gull, *Phys. Rev. X* **5**, 041041 (2015).
- [4] S. R. White, *Phys. Rev. Lett.* **69**, 2863 (1992).
- [5] U. Schollwöck, *Rev. Mod. Phys.* **77**, 259 (2005).
- [6] E. Y. Loh, J. E. Gubernatis, R. T. Scalettar, S. R. White, D. J. Scalapino, and R. L. Sugar, *Phys. Rev. B* **41**, 9301 (1990).
- [7] W. M. C. Foulkes, L. Mitas, R. J. Needs, and G. Rajagopal, *Rev. Mod. Phys.* **73**, 33 (2001).
- [8] M. Troyer and U.-J. Wiese, *Phys. Rev. Lett.* **94**, 170201 (2005).
- [9] E. Fradkin, S. A. Kivelson, and J. M. Tranquada, *Rev. Mod. Phys.* **87**, 457 (2015).
- [10] Michael Nielsen, *Neural Networks and Deep Learning* (Free Online Book, 2013).
- [11] Y. LeCun, Y. Bengio, and G. Hinton, *Nature* **521**, 436 (2015).
- [12] M. Jordan and T. Mitchell, *Science* **349**, 255 (2015).
- [13] G. Torlai, G. Mazzola, J. Carrasquilla, M. Troyer, R. Melko, and G. Carleo, *Nature Physics* **14**, 447 (2018).
- [14] J. Carrasquilla, G. Torlai, R. G. Melko, and L. Aolita, *Nat. Mach. Intell.* **1**, 155 (2019).
- [15] L. Wang, *Phys. Rev. B* **94**, 195105 (2016).
- [16] J. Carrasquilla and R. G. Melko, *Nature Physics* **13**, 431 (2017).
- [17] Y. Zhang and E.-A. Kim, *Phys. Rev. Lett.* **118**, 216401 (2017).
- [18] K. Ch'ng, J. Carrasquilla, R. G. Melko, and E. Khatami, *Phys. Rev. X* **7**, 031038 (2017).
- [19] P. Broecker, J. Carrasquilla, R. G. Melko, and S. Trebst, *Scientific Reports* **7**, 8823 (2017).
- [20] Y. Zhang, R. G. Melko, and E.-A. Kim, *Phys. Rev. B* **96**, 245119 (2017).
- [21] P. Zhang, H. Shen, and H. Zhai, *Phys. Rev. Lett.* **120**, 066401 (2018).
- [22] W. Lian, S.-T. Wang, S. Lu, Y. Huang, F. Wang, X. Yuan, W. Zhang, X. Ouyang, X. Wang, X. Huang, L. He, X. Chang, D.-L. Deng, and L. Duan, *Phys. Rev. Lett.* **122**, 210503 (2019).
- [23] G. Carleo and M. Troyer, *Science* **355**, 602 (2017).
- [24] D.-L. Deng, X. Li, and S. Das Sarma, *Phys. Rev. X* **7**, 021021 (2017).
- [25] A. A. Melnikov, H. Poulsen Nautrup, M. Krenn, V. Dunjko, M. Tiersch, A. Zeilinger, and H. J. Briegel, *Proceedings of the National Academy of Sciences* **115**, 1221 (2018).
- [26] Y. Zhang, A. Mesaros, K. Fujita, S. Edkins, M. Hamidian, K. Ch'ng, H. Eisaki, S. Uchida, J. S. Davis, E. Khatami, *et al.*, *Nature* **570**, 484 (2019).
- [27] C. Valagiannopoulos, *Journal of Applied Physics* **127**, 174301 (2020), <https://doi.org/10.1063/5.0006780>.
- [28] Please refer to Supplemental Materials for the details on examples on machine learning quantum constraints for multiple Fermi seas, our constrained optimization methods, generation of training dataset, the settings of our ANNs, and additional results on 1D fermion chains and 1D spin chains, which include Ref. 34–40.
- [29] The arguments can generalize to complex t straightforwardly noting that the minimum energy requires $\arg C_1 = -\arg t$.
- [30] Although the metallic state at $V = 0$ offers a good starting point, the transaction in r and r' may cause issues.
- [31] M. Fannes, B. Nachtergaele, and R. F. Werner, *Communications in Mathematical Physics* **144**, 443 (1992).
- [32] U. Schollwöck, *Annals of Physics* **326**, 96 (2011).
- [33] E. Lieb, T. Schultz, and D. Mattis, *Annals of Physics* **16**, 407 (1961).
- [34] A. Paszke, S. Gross, F. Massa, A. Lerer, J. Bradbury, G. Chanan, T. Killeen, Z. Lin, N. Gimelshein, L. Antiga, A. Desmaison, A. Kopf, E. Yang, Z. DeVito, M. Raison, A. Tejani, S. Chilamkurthy, B. Steiner, L. Fang, J. Bai, and S. Chintala, in *Advances in Neural Information Processing Systems*, Vol. 32, edited by H. Wallach, H. Larochelle, A. Beygelzimer, F. d'Alché-Buc, E. Fox, and R. Garnett (Curran Associates, Inc., 2019).
- [35] J. Han and C. Moraga, in *From Natural to Artificial Neural Computation*, edited by J. Mira and F. Sandoval

- (Springer Berlin Heidelberg, Berlin, Heidelberg, 1995) pp. 195–201.
- [36] K. He, X. Zhang, S. Ren, and J. Sun, in *Proceedings of the IEEE Conference on Computer Vision and Pattern Recognition (CVPR)* (2016).
- [37] K. Fukushima, *IEEE Transactions on Systems Science and Cybernetics* **5**, 322 (1969).
- [38] X. Glorot, A. Bordes, and Y. Bengio, in *Proceedings of the Fourteenth International Conference on Artificial Intelligence and Statistics*, Proceedings of Machine Learning Research, Vol. 15, edited by G. Gordon, D. Dunson, and M. Dudík (PMLR, Fort Lauderdale, FL, USA, 2011) pp. 315–323.
- [39] S. Ioffe and C. Szegedy, “Batch normalization: Accelerating deep network training by reducing internal covariate shift,” (2015), arXiv:1502.03167 [cs.LG].
- [40] J. Hauschild and F. Pollmann, *SciPost Phys. Lect. Notes*, **5** (2018), arXiv:1805.00055.
- [41] Fewer Fermi seas can be represented as identical values in $\{k_n\}$.